Scaling Laws of Polyelectrolyte Adsorption

Itamar Borukhov and David Andelman*

School of Physics and Astronomy, Raymond and Beverly Sackler Faculty of Exact Sciences, Tel-Aviv University, Ramat-Aviv 69978, Tel-Aviv, Israel

Henri Orland

Service de Physique Théorique, CE-Saclay, 91191 Gif-sur-Yvette Cedex, France

Received May 27, 1997; Revised Manuscript Received October 28, 1997

ABSTRACT: Adsorption of charged polymers (polyelectrolytes) from a semidilute solution to a charged surface is investigated theoretically. We obtain simple scaling laws for (i) the amount of polymer Γ adsorbed to the surface and (ii) the width D of the adsorbed layer, as a function of the fractional charge per monomer p and the salt concentration c_b. For strongly charged polyelectrolytes ($p \lesssim 1$) in a low-salt solution, both Γ and D scale as $p^{-1/2}$. In high-salt solutions $D \sim c_b^{1/2}/p$ whereas the scaling behavior of Γ depends on the strength of the polymer charge. For weak polyelectrolytes ($p \ll 1$) we find that $\Gamma \sim p/c_b^{1/2}$, and for strong polyelectrolytes $\Gamma \sim c_b^{1/2}/p$. Our results are in good agreement with adsorption experiments and with numerical solutions of mean-field equations.

I. Introduction

Polyelectrolytes (charged polymers) are widely used in industrial applications. For example, many colloidal suspensions can be stabilized by the adsorption of polyelectrolytes. In many experiments, the total amount of polymer adsorbed on a surface (the polymer *surface excess*) is measured as a function of the bulk polymer concentration, pH and/or ionic strength of the bulk solution.[1−8] (For reviews see, e.g., refs. 9−12). More recently, spectroscopy[3] and ellipsometry[7] have been used to measure the width of the adsorbed polyelectrolyte layer. Other techniques such as neutron scattering can be employed to measure the entire profile of the adsorbed layer.[13,14]

The theoretical treatment of polyelectrolytes in solution is not very well established because of the delicate interplay between the chain connectivity and the long range nature of electrostatic interactions.[15−18] In many studies adsorption of polyelectrolytes is treated as an extension of neutral polymer theories. In these approaches the polymer concentration profile is determined by minimizing the overall free energy.

One approach is a discrete *multi-Stern layer* model,[19−23] in which the system is placed on a lattice whose sites can be occupied by a monomer, a solvent molecule, or a small ion. The electrostatic potential is determined self-consistently together with the concentration profiles of the polymer and the small ions. Another approach treats the electrostatic potential and the polyelectrolyte concentration as continuous functions.[24−28] These quantities are obtained from two coupled differential equations derived from the total free energy of the system.

In the present work we focus on the adsorption behavior of polyelectrolytes near a single charged surface held at a constant potential. Simple scaling expressions are presented and compared to concentration profiles that we obtain from exact numerical solutions, and to experiments measuring the amount of polymer adsorbed on the surface. In section I the adsorption problem is treated numerically. We then present in section II simple scaling arguments describing the adsorption characteristics and, in section III, we compare our scaling results to experiments. Finally, we present our conclusions and some future prospects.

II. Numerical Profiles

Consider a semi-dilute solution of polyelectrolytes in good solvent in contact with a charged surface (Figure 1). In addition to the polymer chains and their counterions, the solution contains small ions (salt) assumed hereafter to be monovalent. The system is coupled to a bulk reservoir containing polyelectrolyte chains and salt. In the present work we assume that the charge density on the polymer chains is continuous and uniformly distributed along the chains. This assumption is valid as long as the electrostatic potential is not too high, $|\beta e\psi| < 1$, where $1/\beta = k_B T$ is the thermal energy, e is the electron charge, and ψ is the electrostatic potential. Further treatments of the polymer charge distribution (annealed and quenched models) can be found in refs. 27 and 28.

Within mean-field approximation, the free energy of the system can be expressed in terms of the local electrostatic potential $\psi(\mathbf{r})$, the local monomer concentration $c(\mathbf{r})$ and the local concentration of positive and negative ions $c^{\pm}(\mathbf{r})$. It is convenient to introduce the polymer order parameter $\phi(\mathbf{r})$ where $c(\mathbf{r}) = |\phi(\mathbf{r})|^2$. The excess free energy with respect to the bulk is then[25−28]

$$F = \int \mathrm{d}\mathbf{r}\, \{f_{\mathrm{pol}}(\mathbf{r}) + f_{\mathrm{ions}}(\mathbf{r}) + f_{\mathrm{el}}(\mathbf{r})\} \tag{1}$$

The polymer contribution is

$$f_{\mathrm{pol}}(\mathbf{r}) = k_B T\left[\frac{a^2}{6}|\nabla\phi|^2 + \frac{1}{2}v(\phi^4 - \phi_b^4)\right] - \mu_p(\phi^2 - \phi_b^2) \tag{2}$$

where the first term is the polymer elastic energy, a being the effective monomer size. The second term is the excluded volume contribution where v is of order a^3. The last term couples the system to the reservoir, where μ_p is the chemical potential of the polymers and $c(\infty) = \phi_b^2$ is the bulk monomer concentration.

S0024-9297(97)00730-4 CCC: $15.00
Published on Web 02/13/1998

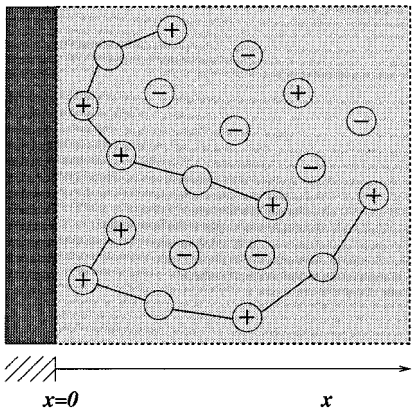

Figure 1. Schematic view of a polyelectrolyte solution in contact with a flat surface at $x = 0$. The solution contains polyelectrolyte chains and small ions. In our model, the surface is held at a constant potential.

The entropic contribution of the small (monovalent) ions is

$$f_{\text{ions}}(\mathbf{r}) = \sum_{i=\pm} k_B T[c^i \ln c^i - c^i - c_b^i \ln c_b^i + c_b^i] - \mu^i(c^i - c_b^i) \quad (3)$$

where $c^i(\mathbf{r})$, c_b^i, and μ^i are, respectively, the local concentration, the bulk concentration, and the chemical potential of the $i = \pm$ ions. Finally, the electrostatic contributions are

$$f_{\text{el}}(\mathbf{r}) = pe\phi^2\psi + ec^+\psi - ec^-\psi - \frac{\epsilon}{8\pi}|\nabla\psi|^2 \quad (4)$$

The first three terms are the electrostatic energies of the monomers, the positive ions, and the negative ions, respectively, p being the fractional charge carried by one monomer. The last term is the self energy of the electric field where ϵ is the dielectric constant of the solution. Note that the electrostatic contribution, eq 4 is equivalent to the well known result: $F_{\text{el}} = (\epsilon/8\pi) \int d\mathbf{r}|\nabla\psi|^2$ plus surface terms. This can be seen by substituting the Poisson–Boltzmann equation (as obtained below) into eq 4 and then integrating by parts.

Minimization of the free energy with respect to $c^{\pm}$, ϕ, and ψ yields a Boltzmann distribution for the density of the small ions, $c^{\pm}(\mathbf{r}) = c_b^{\pm} \exp(\mp\beta e\psi)$, and two coupled differential equations for ϕ and ψ:

$$\nabla^2\psi(\mathbf{r}) = \frac{8\pi e}{\epsilon} c_b \sinh(\beta e\psi) - \frac{4\pi e}{\epsilon}(p\phi^2 - p\phi_b^2 e^{\beta e\psi}) \quad (5)$$

$$\frac{a^2}{6}\nu\phi(\mathbf{r}) = \nu(\phi^3 - \phi_b^2\phi) + p\phi\beta e\psi \quad (6)$$

Equation 5 is a generalized Poisson–Boltzmann equation including the free ions as well as the charged polymers. The first term represents the salt contribution and the second term is due to the charged monomers and their counterions. Equation 6 is a generalization of the self-consistent field equation of neutral polymers.[16] In the bulk, the above equations are satisfied by setting $\psi \to 0$ and $\phi \to \phi_b$.

When a polyelectrolyte solution is in contact with a charged surface, the chains adsorb to (or deplete from) the surface, depending on the nature of the monomer–surface interactions. The large number of monomers on each polymer chain enhances these interactions. For simplicity, we assume that the surface is ideal, i.e., flat and homogeneous. In this case physical quantities depend only on the distance x from the surface (see Figure 1). The surface imposes boundary conditions on the polymer order parameter $\phi(x)$ and electrostatic potential $\psi(x)$. In thermodynamic equilibrium all charge carriers in solution should exactly balance the surface charges (charge neutrality). The Poisson–Boltzmann equation (eq 5), the self-consistent field equation (eq 6) and the boundary conditions uniquely determine the polymer concentration profile and the electrostatic potential. In most cases, these two coupled nonlinear equations can only be solved numerically.

In the present work we have chosen the surface to be at a constant potential ψ_S, leading to the following electrostatic boundary condition

$$\psi|_{x=0} = \psi_S \quad (7)$$

The boundary conditions for $\phi(x)$ depend on the nature of the short range interaction of the monomers and the surface. For simplicity, we take a nonadsorbing surface and require that the monomer concentration will vanish there:

$$\phi|_{x=0} = 0 \quad (8)$$

The choice of boundary conditions depends on the physical system considered. From the numerical point of view other boundary conditions which include the first derivatives of ψ and ϕ can be implemented as well. Possible variations of these boundary conditions include surfaces with a constant surface charge[29] and surfaces with a nonelectrostatic short range attractive (or repulsive) interaction with the polymer.

Far from the surface ($x \to \infty$) both ψ and ϕ reach their bulk values and their derivatives vanish: $\psi'|_{x\to\infty} = 0$ and $\phi'|_{x\to\infty} = 0$.

The numerical solutions of the mean-field equations (eqs 5 and 6) together with the boundary conditions discussed above are obtained using a minimal square method. In this method, the spatial coordinate x is discretized up to a certain distance far enough from the surface. An error functional is then calculated by summing up the squares of the errors in the two mean-field equations at each mesh point. This functional is then minimized under the constraint that the boundary conditions are satisfied.

In Figure 2 several adsorption profiles calculated numerically are plotted. The polymer is positively charged and is attracted to the nonadsorbing surface held at a constant negative potential. The aqueous solution contains a small amount of monovalent salt ($c_b =$ 0.1 mM). The reduced concentration profile $c(x)/\phi_b^2$ is plotted as a function of the distance from the surface x. Different curves correspond to different values of the reduced surface potential $y_S = \beta e\psi_S$, the charge fraction p, and the monomer size a. Although the spatial variation of the profiles differs in detail, they all have a single peak which can be characterized by its height and width. We use this feature in the next section to obtain simple analytical expressions characterizing the adsorption.

III. Scaling Results

The difficulty in obtaining a simple picture of polyelectrolyte adsorption lies in the existence of several

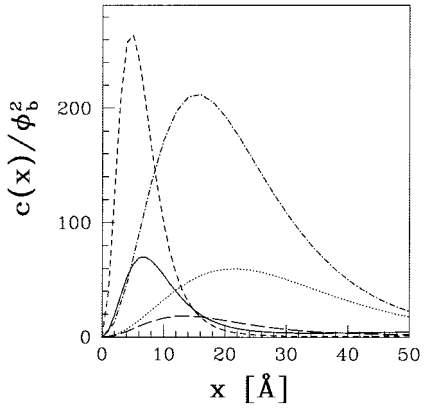

Figure 2. Adsorption profiles obtained by numerical solutions of eqs 5 and 6 for several sets of physical parameters in the low-salt limit. The polymer concentration scaled by its bulk value ϕ_b^2 is plotted as a function of the distance from the surface. The different curves correspond to: $p = 1$, $a = 5$ Å, and $y_S = \beta e \psi_S = -0.5$ (solid curve); $p = 0.1$, $a = 5$ Å, and $y_S = -0.5$ (dots); $p = 1$, $a = 5$ Å, and $y_S = -1.0$ (short dashes); $p = 1$, $a = 10$ Å, and $y_S = -0.5$ (long dashes); and $p = 0.1$, $a = 5$ Å, and $y_S = 1.0$ (dot−dash line). For all cases $\phi_b^2 = 10^{-6}$ Å^{-3}, $v = 50$ Å^3, $\epsilon = 80$, $T = 300$ K, and $c_b = 0.1$ mM.

length scales in the problem: (i) the Edwards correlation length $\xi = a/(v\phi_b^2)^{1/2}$, characterizing the concentration fluctuations of neutral polymer solutions; (ii) the Debye−Hückel screening length $\kappa_s^{-1} = (8\pi l_B c_b)^{-1/2}$ where $l_B = e^2/\epsilon k_B T$ is the Bjerrum length equal to about 7 Å for aqueous solutions at room temperature. Additional length scales can be associated with electrostatic and/or short range surface interactions.

Motivated by the numerical results (Figure 2), we assume that the balance between these interactions results in one dominant length scale D characterizing the adsorption at the surface. Hence, we write the polymer order parameter profile in the form

$$\phi(x) = \sqrt{c_m}\, h(x/D) \tag{9}$$

where h is a dimensionless function normalized to unity at its maximum and c_m sets the scale of polymer adsorption. The free energy can be now expressed in terms of D and c_m, while the exact form of $h(z)$ affects only the numerical prefactors.

In principle, the adsorption length D depends also on the ionic strength through κ_s^{-1}. As discussed below the scaling assumption (eq 9) is only valid as long as κ_s^{-1} and D are not of the same order of magnitude. Otherwise, h should be a function of both $\kappa_s x$ and x/D. We concentrate now on two limiting regimes where eq 9 can be justified: (i) the low-salt regime $D \ll \kappa_s^{-1}$ and (ii) the high-salt regime $D \gg \kappa_s^{-1}$.

Low-Salt Regime: $D \ll \kappa_s^{-1}$. In the low-salt regime the effect of the small ions can be neglected and the free energy, eqs 1−4, is approximated by (see also ref 26)

$$\beta F = A_1 \frac{a^2}{6D} c_m - A_2 p |y_S| c_m D + 4\pi B_1 l_B p^2 c_m^2 D^3 + \frac{1}{2} B_2 v c_m^2 D \tag{10}$$

The first term is the elastic energy characterizing the response of the polymer to concentration inhomogeneities. The second term accounts for the electrostatic attraction of the polymers to the charged surface. The third term represents the Coulomb repulsion between adsorbed monomers. Indeed, the interaction between two layers with charge densities per unit area $\sigma = pe\phi^2(x)dx$ and $\sigma' = pe\phi^2(x')dx'$, is proportional to their distance $|x - x'|$ and yields the D^3 dependence. The last term represents the excluded volume repulsion between adsorbed monomers, where we assume that the monomer concentration near the surface is much larger than the bulk concentration $c_m \gg \phi_b^2$. The coefficients A_1, A_2, B_1, and B_2 are numerical prefactors, which depend on the exact shape of the dimensionless function $h(z)$. These coefficients can be explicitly calculated for a specific profile by integrating the Poisson equation without taking into account the small ion contributions.[31] For a linear profile, $h(z) = z$ for $0 \le z \le 1$ and $h(z) = 0$ for $z > 1$, we get $A_1 = 1$, $A_2 = 1/3$, $B_1 = 1/14$, and $B_2 = 1/5$; for a parabolic profile, $h(z) = 4z(1 - z)$ for $0 \le z \le 1$ and $h(z) = 0$ for $z > 1$, we get $A_1 = 16/3$, $A_2 = 8/15$, $B_1 \simeq 1/9$ and $B_2 \simeq 2/5$.

In the low-salt regime and for strong enough polyelectrolytes the electrostatic interactions are much stronger than the excluded volume interactions. Neglecting the latter interactions and minimizing the free energy with respect to D and c_m gives:

$$D^2 = \left(\frac{5A_1}{6A_2}\right) \frac{a^2}{p|y_S|} \sim \frac{1}{p|y_S|} \tag{11}$$

and

$$c_m = \left(\frac{12A_2^2}{25A_1B_1}\right) \frac{|y_S|^2}{4\pi l_B a^2} \sim |y_S|^2 \tag{12}$$

As discussed above, these expressions are valid as long as (i) $D \ll \kappa_s^{-1}$ and (ii) the excluded volume term in eq 10 is negligible. Condition (i) translates into $c_b \ll p|y_S|/(8\pi l_B a^2)$. For $|y_S| \simeq 1$, $a = 5$ Å and $l_B = 7$ Å, this limits the salt concentration to $c_b/p \ll 0.4$ M. Condition (ii) on the magnitude of the excluded volume term can be shown to be equivalent to $p \gg v|y_S|/l_B a^2$. These requirements are consistent with the data presented in Figure 2.

We recall that the profiles presented in Figure 2 were obtained from the numerical solution of eqs 5 and 6, including the effect of small ions and excluded volume. The scaling relations are verified by plotting in Figure 3 the same sets of data as in Figure 2 using rescaled variables as defined in eqs 11 and 12. Namely, the rescaled electrostatic potential $\psi(x)/\psi_S$ and polymer concentration $c(x)/c_m \sim c(x)a^2/|y_S|^2$ are plotted as functions of the rescaled distance $x/D \sim xp^{1/2}|y_S|^{1/2}/a$. The different curves roughly collapse on the same curve.

Note, however, that although the scaling of the spatial coordinate x with D is satisfactory, the scaling of the concentration $c(x)$ with c_m is not as good, especially at the peak. Naturally, our simple scaling approach is expected to lose some of the local details and give a better description of global properties, and in particular the amount of polymer drawn to the surface. In many experiments the total amount of adsorbed polymer per unit area Γ is measured as a function of the physical characteristics of the system such as the charge fraction p, the pH of the solution or the salt concentration c_b.[1−8] This quantity can be easily obtained from our scaling expressions yielding

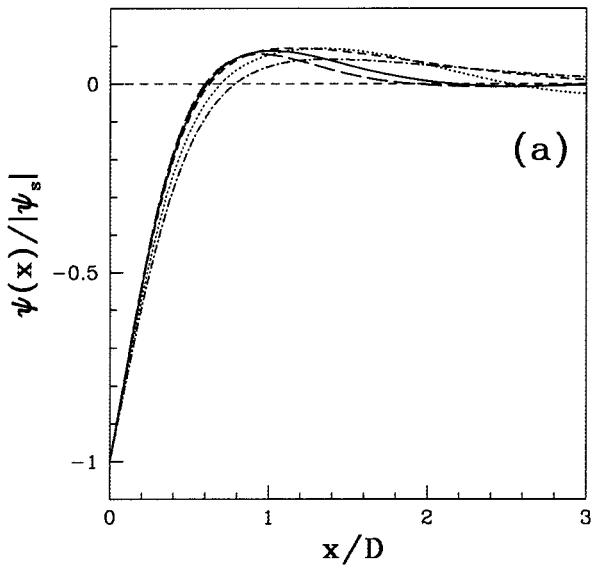

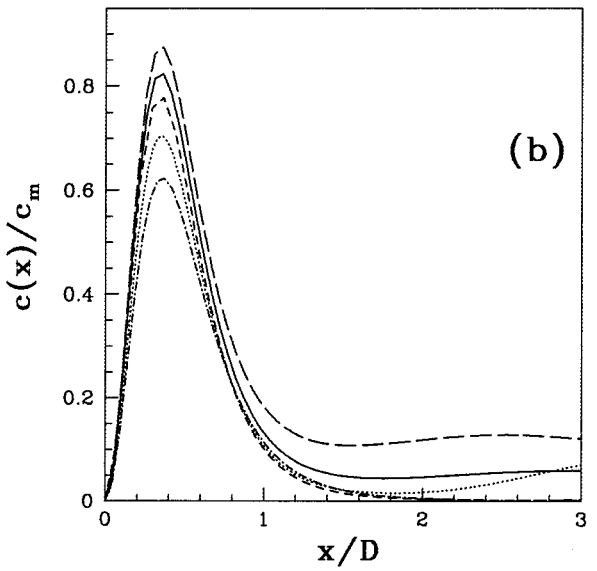

Figure 3. Scaling behavior of polyelectrolyte adsorption in the low-salt regime (eqs 11 and 12). (a) The rescaled electrostatic potential $\psi(x)/|\psi_S|$ as a function of the rescaled distance x/D. (b) The rescaled polymer concentration $c(x)/c_m$ as a function of the same rescaled distance. The profiles are taken from Figure 2 (with the same notation). The numerical prefactors of the linear $h(x/D)$ profile were used in the calculation of D and c_m.

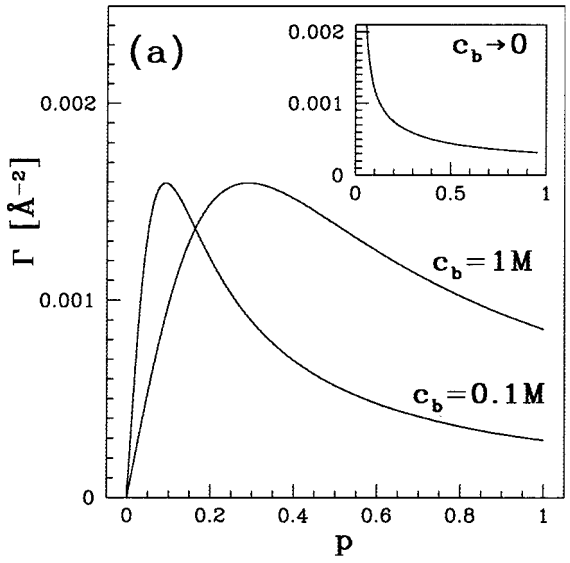

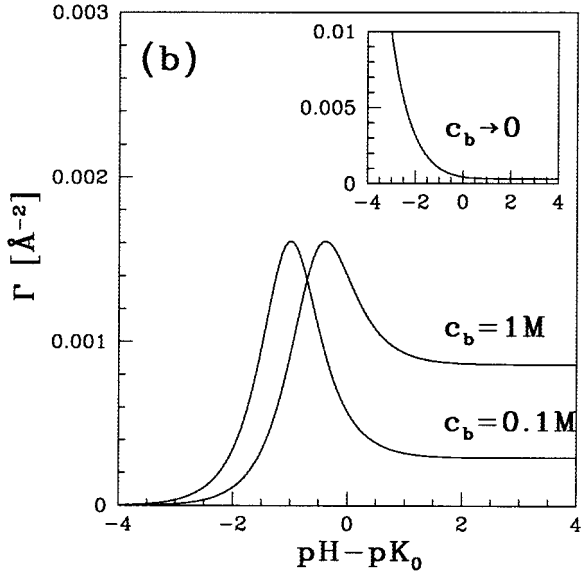

Figure 4. Typical adsorbed amount Γ as a function of (a) the charge fraction p and (b) the pH − pK_0 of the solution for different salt concentrations (eq 17). The insets correspond to the low-salt regime (eq 13). The parameters used for ϵ, T, and v are the same as in Figure 2, and $y_S = -0.5$ and $a = 5$ Å. The bulk concentration ϕ_b^2 is assumed to be much smaller than c_m. The numerical prefactors of the linear $h(x/D)$ were used.

$$\Gamma = \int_0^\infty [c(x) - \phi_b^2]dx \simeq Dc_m \simeq \frac{|y_S|^{3/2}}{l_B a p^{1/2}} \sim \frac{|y_S|^{3/2}}{p^{1/2}} \quad (13)$$

The adsorbed amount $\Gamma(p)$ in the low-salt regime is plotted in the inset of Figure 4a. As a consequence of eq 13, Γ decreases with increasing charge fraction p. Similar behavior was also reported in experiments.[4] This effect is nontrivial, because as the polymer charge increases, the chains are subject to a stronger attraction to the surface. On the other hand, the monomer−monomer repulsion is stronger and indeed, in this regime, the monomer−monomer Coulomb repulsion scales as $(pc_m)^2$, and dominates over the adsorption energy which scales as pc_m.[32]

High-Salt Regime: $D \gg \kappa_s^{-1}$. The opposite case occurs when D is much larger than κ_s^{-1}. In this case the electrostatic interactions are short ranged with a cutoff κ_s^{-1}. The free energy then reads:

$$\beta F = A_1 \frac{a^2}{6D} c_m - A_2 p|y_S| c_m \kappa_s^{-1} + 4\pi B_1 l_B p^2 \kappa_s^{-2} c_m^2 D + \frac{1}{2} B_2 v c_m^2 D \quad (14)$$

The electrostatic cutoff enters in two places. In the second term only the first layer of width κ_s^{-1} interacts electrostatically with the surface. In the third term each charged layer situated at point x interacts only with layers at x' for which $|x - x'| < \kappa_s^{-1}$. Since the interaction between two charged layers at x and x' is proportional to $|x - x'|$, the integral over x' contributes to the κ_s^{-2} dependence, and the integral over x contributes an additional factor of D. This term can be also

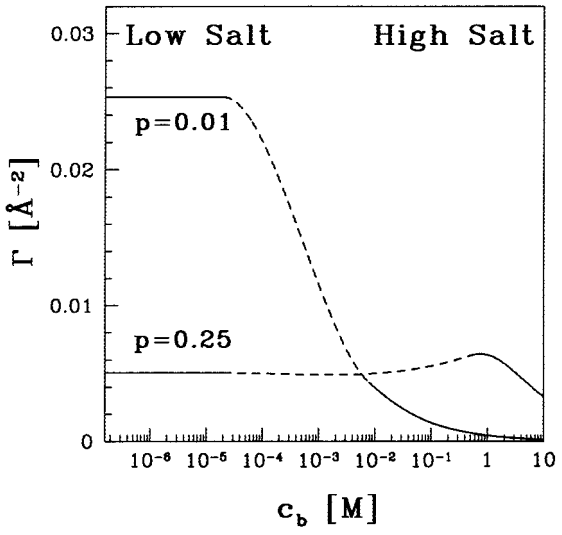

Figure 5. The adsorbed amount Γ as a function of the salt concentration c_b for $p = 0.01$ and 0.25. The solid curves on the right side correspond to the scaling relations in the high-salt regime (eq 17). The horizontal lines on the left side mark the low-salt values (eq 13). The dashed lines serve as guides to the eye. The parameters used are $\epsilon = 80$, $T = 300$ K, $v = 50$ Å^3, $a = 5$ Å, and $y_S = -2.0$ and the numerical prefactors of the linear $h(x/D)$.

viewed as an additional electrostatic excluded volume with $v_{el} \sim l_B(p/\kappa_s)^2$. The crude box-like simplification of screening can be justified when the screening length κ_s^{-1} is much smaller than the adsorption length D, and affects only the numerical factors A_2 and B_1.

Minimization of the free energy gives

$$D = \left(\frac{A_1}{2A_2}\right)\frac{\kappa_s a^2}{p|y_S|} \sim \frac{c_b^{1/2}}{p|y_S|} \tag{15}$$

and

$$c_m \sim \frac{p^2|y_S|^2/(\kappa_s a)^2}{B_1 p^2/c_b + B_2 v} \tag{16}$$

yielding

$$\Gamma \sim \frac{p|y_S|c_b^{-1/2}}{B_1 p^2/c_b + B_2 v} \tag{17}$$

The adsorption behavior is depicted in Figures 4 and 5. Our results are in agreement with numerical solutions of discrete lattice models (the multi-Stern layer theory).[9−11,19−23] In Figure 4, Γ is plotted as function of p (Figure 4a) and the pH (Figure 4b) for different salt concentrations. The behavior as seen in Figure 4b represents annealed polyelectrolytes where the nominal charge fraction is controlled by the pH of the solution through

$$p = \frac{10^{\mathrm{pH}-\mathrm{pK_0}}}{1 + 10^{\mathrm{pH}-\mathrm{pK_0}}} \tag{18}$$

where $\mathrm{pK_0} = -\log_{10}K_0$ and K_0 is the apparent dissociation constant.

Another observation which can be deduced from eq 17 is that Γ is only a function of $p/c_b^{1/2}$. Indeed, as can be seen in Figure 4, c_b only affects the position of the peak and not its height.

The effect of salt concentration is shown in Figure 5, where Γ is plotted as function of the salt concentration c_b for two charge fractions $p = 0.01$ and 0.25. The curves on the right side of the graph are calculated from the high-salt expression for Γ (eq 17). The horizontal lines on the left side of the graph indicate the low-salt values of Γ (eq 13). The dashed lines in the intermediate salt regime serve only as guides to the eye since our approach is not valid when D and κ_s^{-1} are of the same order. The behavior in this regime can be deduced qualitatively by comparing the low-salt asymptotic values with the high-salt values. The effect of salt in the intermediate regime depends strongly on the polymer charge fraction p. For weak polyelectrolytes (e.g., $p = 0.01$) Γ should vary considerably across the intermediate regime, and is expected to decrease as salt is added to the solution. On the other hand, for strong polyelectrolytes (e.g., $p = 0.25$), the adsorbed amount does not change much across this regime.

Attention should be drawn to the distinction between weak and strong polyelectrolytes. For weak polyelectrolytes, the adsorbed amount Γ is a monotonously decreasing function of the salt concentration c_b in the whole range of salt concentrations. The reason being that the monomer−monomer Coulomb repulsion, proportional to p^2, is weaker than the monomer−surface interaction, which is linear in p.

For strong polyelectrolytes, on the other hand, the balance between these two electrostatic terms depends on the amount of salt. At low salt concentrations, the dominant interaction is the monomer−surface Coulomb repulsion. Consequently, addition of salt screens this interaction and increases the adsorbed amount. When the salt concentration is high enough, this Coulomb repulsion is screened out and the effect of salt is to weaken the surface attraction. At this point the adsorbed amount starts to decrease. As a result, the behavior over the whole concentration range is nonmonotonic with a maximum at some optimal value c_b* as seen in Figure 5.

From this analysis and from Figures 4 and 5 and eq 17, it is now natural to divide the high-salt regime into two sub regimes according to the polyelectrolyte charge. At low charge fractions (subregime HS I), $p \ll p^* = (c_b v)^{1/2}$, the excluded volume term dominates the denominator of eq 17 and

$$\Gamma \sim \frac{p|y_S|}{c_b^{1/2}} \tag{19}$$

whereas at high p (subregime HS II), $p \gg p^*$, the monomer−monomer electrostatic repulsion dominates and Γ decreases with p and increases with c_b:

$$\Gamma \sim \frac{c_b^{1/2}\,|y_S|}{p} \tag{20}$$

The various regimes with their crossover lines are shown schematically in Figure 6. Keeping the charge fraction p constant while changing the amount of salt corresponds to a vertical scan through the diagram. For weak polyelectrolytes this cut goes through the left side of the diagram starting from the low-salt regime and, upon addition of salt, into the HS I regime. Such a path describes the monotonous behavior inferred from Figure

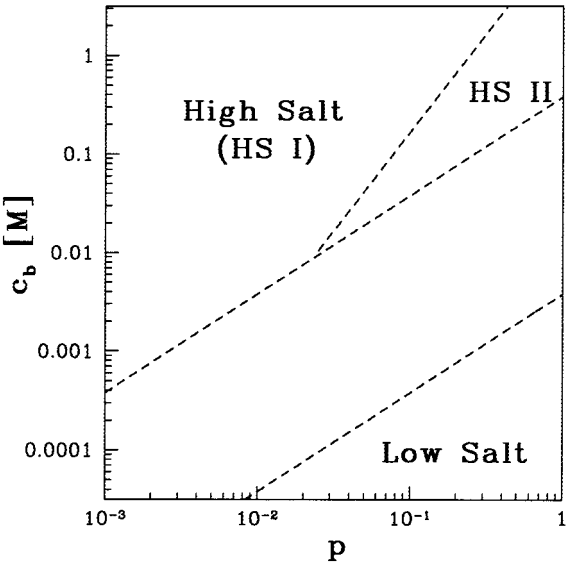

Figure 6. Schematic diagram of the different adsorption regimes as a function of the charge fraction p and the salt concentration c_b. Three regimes can be distinguished: (i) the low-salt regime $D \ll \kappa_s^{-1}$; (ii) the high-salt regime (HS I) $D \gg \kappa_s^{-1}$ for weak polyelectrolytes $p \ll p^* = (c_b v)^{1/2}$; and (iii) the high-salt regime (HS II) $D \gg \kappa_s^{-1}$ for strong polyelectrolytes $p \gg p^*$.

5 for the weak polyelectrolyte ($p = 0.01$). For strong polyelectrolytes the cut goes through the right side of the diagram, starting from the low-salt regime, passing through the HS II regime, and ending in the HS I regime. The passage through the HS II regime is responsible for the nonmonotonous behavior inferred from Figure 5 for the strong polyelectrolyte ($p = 0.25$).

Similarly, Figures 4a and b correspond to horizontal scans through the top half of the diagram. As long as the system is in the HS I regime, the adsorbed amount increases when the polymer charge fraction increases. As the polymer charge further increases, the system enters the HS II regime and the adsorbed amount decreases. Thus, the nonmonotonous behavior of Figure 4 is exhibited.

IV. Comparison to Experiments

In the previous section the adsorption behavior was divided into three distinct regimes (Figure 6): (i) low-salt regime $c_b \ll p|y_S|/8\pi l_B a^2$; (ii) first high-salt (HS I) regime, where $c_b \gg p|y_S|/8\pi l_B a^2$ and $p \ll p^* = (c_b v)^{1/2}$ (weak polyelectrolytes); and (iii) second high-salt (HS II) regime, where $c_b \gg p|y_S|/8\pi l_B a^2$ and $p \gg p^*$ (strong polyelectrolytes).

In the low salt regime $\Gamma \sim |y_S|^{3/2}/p^{1/2}$. In the two HS regimes Γ scales differently $\Gamma \sim p|y_S|/c_b^{1/2}$ in the HS I regime, and $\Gamma \sim c_b^{1/2}|y_S|/p$ in the HS II regime. In the following we compare our results with experimental measurements done on different types of polyelectrolytes and using different experimental techniques. Our scaling results are in good agreement with adsorption experiments, although in real systems the charge distribution of the polyelectrolytes can be more complicated than in our simple model.

Low-Salt Regime. Denoyel et al.[4] have studied the adsorption of heteropolymers made of neutral (acrylamide) and cationic monomers (derived from chloride acrylate). The fractional charge was fixed during the polymerization process and varied from $p = 0$ to 1. Because the salt amount in their experiment was quite low, 1.2 mM corresponding to $\kappa_s^{-1} \simeq 90$ Å, their experimental range satisfies the low-salt conditions. Indeed, the measured Γ (Table 2 in ref 4) exhibits a $p^{-1/2}$ dependence as in eq 13.

Weak Polyelectrolytes: Effect of Salt. Shubin and Linse[7] adsorbed another cationic derivative of polyacrylamide on silica. The fractional charge was fixed at a low value ($p = 0.034$), and the salt concentration varied from $c_b = 0.1$ mM to $c_b \approx 0.2$ M. Ellipsometry was used to measure Γ and D of the adsorbed layer as function of the salt concentration. This low charge fraction belongs to the left side (low p) of Figure 6. The experimental behavior is similar to our predictions as shown in Figure 5 for weak polyelectrolytes. At low electrolyte concentration ($c_b < 1$ mM), the adsorbed amount is essentially constant and decreases at higher salt concentration (HS I regime of Figure 6). Similar behavior was obtained both by numerical calculations using the multi-Stern layer model,[7,22,23] and in other adsorption experiments of cationic potato starch.[6]

Strong Polyelectrolytes: Effect of Salt. Kawaguchi et al.[2] measured the adsorption of a highly charged polyelectrolyte poly(4-vinyl-*N*-*n*-propylpyridinium bromide) (PVPP) on silica surfaces. Because of the high ionic strength this system belongs to the HS II regime. Indeed, Γ scales as $c_b^{1/2}$ was in agreement with our prediction. Meadows et al.[3] also performed adsorption experiments with highly charged ($p = 0.9$) hydrolyzed polyacrylamide. The adsorbed amount Γ and the width of the adsorbed layer D were found to increase upon addition of salt. Qualitatively, this agrees with our prediction in the HS II regime. However, the measured power laws are weaker than our predictions. A simple power law fit of their salt dependence gives $\Gamma \sim c_b^{1/4}$ as compared to our $c_b^{1/2}$ prediction. This behavior is intermediate between the salt free and HS II regimes.

Effect of Charge Fraction. Peyser and Ullman[1] studied the adsorption of poly-4-vinylpyridine (PVP) on a glass surface as a function of the charge fraction for three different salt concentrations. The system belongs to the right side ($p \lesssim 1$) of Figure 6 between the low-salt and HS II regimes. As expected Γ increases with c_b and decreases with p. Moreover, it is possible to fit the data to a simple scaling law of the form $\Gamma \sim c_b^{1/4}/p^{1/2}$. Our scaling results do not fit very well these experiments which lie in the intermediate regime, between the low-salt and HS II regimes.

In experiments on annealed polyelectrolytes,[5,8] the polymer charge can be tuned by the pH of the solution (eq 18). The behavior then shifts continuously from the HS I to the HS II regimes. For example, Blaakmeer et al.[5] used polyacrylic acid which is neutral (no dissociation) at low pH but becomes negatively charged (strong dissociation) at higher pH. As predicted by eq 17 (see also Figure 4b), a nonmonotonous dependence of Γ on the pH was observed, with a maximum below the pK_0. This effect had been already verified by numerical calculations based on the multi-Stern layer model.[5]

A similar maximum in Γ was also observed in adsorption experiments of proteins[12] and diblock copolymers with varying ratios between the charged and neutral blocks[8] and may be interpreted using similar considerations.

V. Conclusions

In this work we used simple arguments to derive scaling laws describing the adsorption of polyelectrolytes on a single charged surface held at a constant potential. We obtained expressions for the amount of adsorbed polymer Γ and the width D of the adsorbed layer, as a function of the fractional charge p and the salt concentration c_b. In the low-salt regime, a $p^{-1/2}$ dependence of Γ is found. It is supported by our numerical solutions of the profile, eqs 5 and 6, and is in agreement with the experiment.[4] This behavior is due to strong Coulomb repulsion between adsorbed monomers in the absence of salt. As p decreases, the adsorbed amount increases until the electrostatic attraction becomes weaker than the excluded volume repulsion, at which point Γ starts to decrease rapidly. At high salt concentrations we obtain two limiting behaviors: (i) for weak polyelectrolytes, $p \ll p^* = (c_b\upsilon)^{1/2}$, the adsorbed amount increases with the fractional charge and decreases with the salt concentration, $\Gamma \sim p/c_b^{1/2}$, because of the monomer−surface electrostatic attraction. (ii) For strong polyelectrolytes, $p \gg p^*$, the adsorbed amount decreases with the fractional charge and increases with the salt concentration, $\Gamma \sim c_b^{1/2}/p$, because of the dominance of the monomer−monomer electrostatic repulsion. Between these two regimes we find that the adsorbed amount reaches a maximum in agreement with other experiments.[5,8]

The scaling approach can serve as a starting point for further investigations. Special attention should be directed to the crossover regime where D and κ_s^{-1} are of comparable size. At present, it is not clear whether the intermediate regime represents simply a crossover between regimes or is a scaling regime on its own. Another important question addresses the relative importance of attractive versus repulsive forces between two charged surfaces in the presence of a polyelectrolyte solution. Finally, our approach could be used in nonplanar geometries such as spheres (colloidal particles) and cylinders.

Acknowledgment. We would like to thank L. Auvray, M. Cohen-Stuart, J. Daillant, H. Diamant, P. Guenoun, Y. Kantor, P. Linse, P. Pincus, S. Safran and C. Williams for useful discussions. Two of us (I.B. and D.A.) would like to thank the Service de Physique Théorique (CE-Saclay) and one of us (H.O.) would like to thank the Sackler Institute of Solid State Physics (Tel Aviv University) for their hospitality. Partial support from the German-Israel Foundation (G.I.F) under grant no. I-0197 and the U.S.-Israel Binational Foundation (B.S.F.) under grant No. 94-00291 is gratefully acknowledged.

References and Notes

(1) Peyser, P.; Ullman, R. *J. Polym. Sci. A* **1965**, *3*, 3165.
(2) Kawaguchi, M.; Kawaguchi, H.; Takahashi, A. *J. Colloid Interface Sci.* **1988**, *124*, 57.
(3) Meadows, J.; Williams, P. A.; Garvey, M. J.; Harrop, R.; Phillips, G. O. *J. Colloid Interface Sci.* **1989**, *132*, 319.
(4) Denoyel, R.; Durand, G.; Lafuma, F.; Audbert, R. *J. Colloid Interface Sci.* **1990**, *139*, 281.
(5) Blaakmeer, J.; Böhmer, M. R.; Cohen Stuart, M. A.; Fleer. G. J. *Macromolecules* **1990**, *23*, 2301.
(6) Van de Steeg. H. G. M.; de Keizer, A.; Cohen Stuart, M. A.; Bijsterbosch, B. H. *Colloid Surf. A* **1993**, *70*, 91.
(7) Shubin, V.; Linse, P. *J. Phys. Chem.* **1995**, *99*, 1285.
(8) Hoogeveen, N. G. Ph.D. Thesis, Wageningen Agricultural University, The Netherlands, 1996.
(9) Cohen Stuart, M. A. *J. Phys. France* **1988**, *49*, 1001.
(10) Cohen Stuart, M. A.; Fleer, G. J.; Lyklema, J.; Norde, W.; Scheutjens, J. M. H. M. *Adv. Colloid Interface Sci.* **1991**, *34*, 477.
(11) Fleer, G. J.; Cohen Stuart, M. A.; Scheutjens, J. M. H. M.; Cosgrove, T.; Vincent, B. *Polymers at Interfaces*; Chapman & Hall: London, 1993; chapter 11.
(12) Haynes, C. A.; Norde, W. *Colloid Surf. B* **1994**, *2*, 517.
(13) Auroy, P.; Auvray, L.; Léger, L. *Macromolecules* **1991**, *24*, 2523.
(14) Guiselin, O.; Lee, L. T.; Farnoux, B.; Lapp, A. *J. Chem. Phys.* **1991**, *95*, 4632.
(15) Oosawa, F. *Polyelectrolytes*; Marcel Dekker: New York, 1971.
(16) De Gennes, P. G. *Scaling Concepts in Polymer Physics*; Cornell Univ.: Ithaca, 1979.
(17) Odijk, T. *Macromolecules* **1979**, *12*, 688.
(18) Dobrynin, A. V.; Colby, R. H.; Rubinstein, M. *Macromolecules* **1995**, *28*, 1859.
(19) Van der Schee, H. A.; Lyklema, J. *J. Phys. Chem.* **1984**, *88*, 6661.
(20) Papenhuijzen, J.; Van der Schee, H. A.; Fleer, G. J. *J. Colloid Interface Sci.* **1985**, *104*, 540.
(21) Evers, O. A.; Fleer, G. J.; Scheutjens, J. M. H. M.; Lyklema, J. *J. Colloid Interface Sci.* **1985**, *111*, 446.
(22) Van de Steeg, H. G. M.; Cohen Stuart, M. A.; de Keizer, A.; Bijsterbosch, B. H. *Langmuir* **1992**, *8*, 8.
(23) Linse, P. *Macromolecules* **1996**, *29*, 326.
(24) Muthukumar, M. *J. Chem. Phys.* **1987**, *86*, 7230.
(25) Varoqui, R.; Johner, A.; Elaissari, A. *J. Chem. Phys.* **1991**, *94*, 6873.
(26) Varoqui, R. *J. Phys. II* **1993**, *3*, 1097.
(27) Borukhov, I.; Andelman, D.; Orland, H. *Europhys. Lett.* **1995**, *32*, 499; Borukhov, I.; Andelman, D.; Orland, H. In *Short and Long Chains at Interfaces*; Daillant, J., Guenoun, P., Marques, C., Muller, P., Trân Thanh Vân, J., Eds.; Edition Frontieres: Gif-sur-Yvette, 1995; pp. 13−20.
(28) Borukhov, I.; Andelman, D.; Orland, H. *Eur. Phys. J. D*, submitted for publication.
(29) If a constant surface charge density σ is assumed, the boundary condition then becomes $\psi'|_S = -4\pi\sigma/\epsilon$. In real systems, some of the ionized surface sites can be neutralized by the binding of small ions from the solution. The actual surface charge is not fixed but depends on the surface potential (see also ref. 30). Neither the surface potential nor the surface charge are fixed, and the boundary conditions are mixed. The choice of simple boundary conditions is only an approximation of a real surface−solution system. The quality of the approximation depends on the details of the experimental system.
(30) For a review see: Israelachvili, J. N. *Intermolecular and Surface Forces*, 2nd ed.; Academic Press: London, 1990.
(31) For a given profile $h(x/D)$, the electrostatic potential, which is also a function of x/D, can be calculated by integrating the charge density from the surface up to a distance x. The surface charge density is determined from charge neutrality which is imposed by setting the electric field to zero at $x = D$. The electrostatic term in the free energy f_{el} is then obtained by integrating $pec_m\, h^2(x/D)\psi(x)$.
(32) This behavior is valid for a wide range of p values. However, as $p \to 0$, eventually the excluded volume interaction will take over and Γ will start to decrease to zero.

MA9707300